Application of the boundary face method to solve the 3D acoustic wave problems*

X Wang, J Zhang† F Zhou
State Key Laboratory of Advanced Design and Manufacturing for Vehicle Body,
College of Mechanical and Vehicle Engineering, Hunan University, Changsha, China

ABSTRACT: *The boundary face method based on the Burton-Miller equation is applied in this paper to solve radiation and scattering problem of acoustic waves. The present method is referred to as CHBFM. In the CHBFM, the boundary integration and field variables approximation are both performed in the parametric space of each boundary face exactly the same as the B-rep data structure in standard solid modelling packages. The geometric data, such as coordinates and the outward normals at Gaussian integration points are calculated directly from the faces rather than from element interpolation, thus the geometric errors are avoided. The CHBFM has been integrated into the widely used commercial CAD package UG-NX, and thus able to handle problems with complicated geometries. Numerical examples were presented to illustrate the accuracy and validity of the CHBFM. The results have shown that our method has better accuracy than the traditional method with almost the same CPU time when using the same number of elements. In addition, the CAD models, even with complicated geometry, are directly converted into the CHBFM models, thus the present method provides a new way toward automatic simulation.*

KEYWORDS: Boundary face method; Burton-Miller equation; acoustic wave problems; CAD models.

REFERENCE: Wang, X., Zhang, J. & Zhou, F. 2013, "Application of the boundary face method to solve the 3D acoustic wave problems", *Australian Journal of Mechanical Engineering*, Vol. 11, No. 1.

1 INTRODUCTION

For the acoustic problem governed by Helmholtz equation, the first effort of using the integral equation was made by Jawson & Symm (1963). Chen & Schweikert (1963) solved 3D sound radiation problems by using Fredholm integral equation of the second kind. Chertock (1964) predicted sound radiation from vibrating surfaces using integral equation. However, there is a drawback that only using CBIE formulation cannot get unique solution for the exterior acoustic problems governed by the Helmholtz equation at the eigen-frequencies which are associated with the interior problems (Schenck, 1968; Kleinman & Roach, 1974). These eigen-frequencies, which are called fictitious eigen-frequencies, have no physical significance for the exterior problems under investigation. In order to deal with this defect, two major methods have been applied to circumvent this problem. One is the combined Helmholtz integral equation formulation (CHIEF), which was proposed by Schenck (1968). In that method, some additional Helmholtz integral relations were added in the interior domain. This additional relation leads to an over-determined system of equations, which can be solved using a least-squares technique. CHIEF has been widely used for acoustic scattering and radiation problems. Furthermore, lots of improvements have been made by several researchers (Seybert & Rengarajan, 1987; Wu & Seybert, 1991; Segalman & Lobitz, 1992; Benthien & Schenck, 1997). The main difficulty in this

* Reviewed and revised version of paper presented at the 10th National Engineering Calculation Conference and Global Chinese Workshop on Computational Methods in Engineering, 25-28 May 2012, University of Hunan, Changsha, Hunan, China.

† Corresponding author Prof Jianming Zhang can be contacted at zhangjm@hnu.edu.cn.

method, however, is a suitable choice of number and positions of the interior points.

The other method to circumvent the non-uniqueness problem at characteristic frequencies was proposed by Burton & Miller (1971). In this method, a complex linear combination of the CBIE and hyper-singular boundary integral equation (HBIE) for only the exterior domain is employed. This method was proved to yield a unique solution efficiently for all the frequencies if the imaginary part of the coupling constant of the two equations is non-zero. However, the most difficult part in implementing this composite formulation is calculating the hyper-singular integral. Burton & Miller (1971) proposed a double surface integral method throughout the integral equation to reduce the order of hyper-singularity. Chien et al (1990) used some identities in the integral equation related to an interior Laplace problem to reduce the order of kernel singularity. Based on the three integral identities for the static Green's function which were proposed by Liu & Rudolphi (1991), a weakly singular form of the hyper-singular integral equations was presented by Liu & Rizzo (1992) and Liu & Chen (1999). In those works, the hyper-singular integral is calculated by subtracting a two-term Taylor series from the density function. Certain integral identities of static Green's function were used to assess the added-back terms. In the weakly integral form of the HBIE, all the integrals are at most weakly integral. Thus the ordinary numerical integration scheme can be applied. Rudolphi (1991) obtained a regularised form by using the rigid body and linear displacement modes. Guiggiani (1998) computed the hyper-singular integral directly in the Hadamard-finite-part sense. There are also some other efforts on this aspect have been made for acoustic problems (Meyer et al, 1979; Lee & Sclavounos, 1989; Liu & Rudolphi, 1999; Li & Huang, 2010; Matsumoto et al, 2010).

All the above mentioned works were performed in boundary element method (BEM) frame. In BEM, however, the curved surfaces are approximated through boundary elements. In other words, the calculated geometric curved surface is different from the real one. A large number of elements should usually be employed to get an accurate result in BEM. To circumvent this problem, the boundary face method (BFM) was proposed by Zhang et al (2009). The BFM based on the boundary integral equation (BIE) is also a numerical approach for solving field problems, and it is implemented directly using the boundary representation (B-rep) data structure that is used in most CAD packages for geometry modelling. In BFM, both boundary integration and interpolation of field variables are performed in the parametric space of each boundary face. The geometric data at Gaussian integration points, such as the coordinates, the Jacobians and the outward normals are calculated directly from the faces rather than from element interpolation. Thus the geometric errors are avoided. Qin et al (2010) implemented the BFM using finite elements defined in the parametric space of boundary faces, which can be considered as a new implementation of the BEM. Gu et al (2011) applied the BFM to solve linear elasticity problems using B-spline element interpolation. Zhou et al (2011) combined the dual reciprocity method and the BFM to solve non-homogeneous potential problems. Other applications of BFM can be found in Zhang (2010) and Gu et al (2012).

In this paper, the BFM is implemented based on the Burton-Miller equation to solve the radiation and scattering problems of the acoustic wave. In this implementation, the constant elements are employed. CAD software UG-NX is employed for the geometric design. The paper is organised as follows. Section 2 mainly reviews the BIE for the acoustic wave problems used in this paper. In section 3, the BFM for the BIEs of acoustic wave problems is described followed by several numerical examples in section 4. The paper ends with conclusions and discussions on future work in section 5.

2 REVIEW TO THE FORMULATION OF ACOUSTIC WAVE PROBLEMS

In 2D or 3D spaces, the governing equation for acoustic wave problem is the Helmholtz equation which can be written as:

$$\nabla^2\phi(x) + k^2\phi(x) = 0, \ x \in E \tag{1}$$

in which x is the field point; E is the acoustic domain; $\phi(x)$ denotes the total sound pressure at x; $\nabla^2 = \frac{\partial^2}{\partial^2 x_1} + \frac{\partial^2}{\partial^2 x_2} + \frac{\partial^2}{\partial^2 x_3}$ denotes the Laplace operator, where x_1, x_2 and x_3 are the coordinates; $k = 2\pi f/c$ denotes the wave number; f is the cyclic frequency; and c is the speed of sound in the acoustic medium.

The boundary conditions for the governing equation of acoustic wave problems can be described as:

$$\begin{cases} \text{Dirichlet type} & \phi = \overline{\phi}, & \forall x \in S_u \\ \text{Neumann type} & q = \dfrac{\partial \phi}{\partial n} = \overline{q} = ikc\rho v_n, & \forall x \in S_q \\ \text{Impedance type} & \phi = Z v_n, & \forall x \in S_z \end{cases} \tag{2}$$

where ω denotes the circular frequency; ρ is the mass density; v_n is the normal velocity; n is the outward normal; Z denotes the specific acoustic impedance; $i = \sqrt{-1}$; and the quantities with overbars indicate given values. For the exterior acoustic problem, the Sommerfeld radiation condition must be satisfied at infinite field. It is:

$$\lim_{R \to \infty}\left[R\left|\frac{\partial\phi}{\partial R} - ik\phi\right|\right] = 0 \tag{3}$$

where R is the distance from a fixed origin to a general field point; and ϕ is the radiated wave in a radiation problem or the scattered wave in a scattering problem.

The integral representation of the solution to the Helmholtz equation is:

$$c(P_0)\phi(P_0) = \int_S G(P_0,P)q(P)S(P) - \int_S \frac{\partial G(P_0,P)}{\partial n}\phi(P)dS(P) + \phi^I(P_0) \tag{4}$$

here $G(P_0, P) = e^{ikr}/4\pi r$ denotes the full space Green's function of Helmholtz problems, in which $r = |P - P_0|$ is the distance between source point P_0 and filed point P; $q(P) = \partial\phi(P)/\partial n$; and $\phi^I(P_0)$ denotes a prescribed incident wave but it does not exist in radiation problems. Coefficient $c(P_0)$ is described as:

$$c(P_0) = \begin{cases} 1, & P_0 \in E \\ \frac{1}{2}, & P_0 \in S \\ 0, & P_0 \in B \end{cases} \tag{5}$$

where E is the exterior region (acoustic medium); S denotes the boundary which is smooth around P_0; and B is the interior region (a body or scatterer). Equation (4) with $P_0 \in S$ is the commonly used form of the conventional BIE for acoustic wave problems.

To derive the HBIE, we take the derivative of equatoin (4) with respect to the outward normal n_0 at source point P_0. The following BIE is given:

$$c(P_0)\frac{\partial\phi(P_0)}{\partial n_0} = \int_S \frac{\partial G(P_0,P)}{\partial n_0}\frac{\partial\phi(P)}{\partial n}dS(P) - \int_S \frac{\partial^2 G(P_0,P)}{\partial n \partial n_0}\phi(P)dS(P) + \frac{\partial\phi^I(P_0)}{\partial n_0}, P_0 \in S \tag{6}$$

here $c(P_0)$ is 1/2 if S is smooth around the source point P_0. As we all know, equation (6) is a hyper-singular integral equation (integrand has a $1/r^3$ singularity). Thus the main problem in application of this integral equation is how to calculate the hyper-singular integral accurately. Many regularisation and weakly singular integral forms have been proposed to calculate this integral efficiently, which has been introduced in the previous section. In this paper, we employ the weakly singular integral form proposed by Liu & Chen (1999).

By employing the above formula, all the hyper-singular integral or strong singular integral (integrand has a $1/r^3$ singularity) in the BIE have been converted into weakly singular integral forms which can be calculated directly.

We both convert the BIE and HBIE to their weakly singular form. Then we apply the well-known Burton-Miller equation with a coupling constant β. A weakly singular formed Burton-Miller formulation as follow can be obtained by (Liu & Rizzo, 1992; Liu & Chen, 1999):

$$\text{CBIE} + \beta\text{HBIE} \tag{7}$$

$\beta = i/k$ is used as the imaginary coupling parameter of the Burton-Miller's formulation (Seybert et al, 1985), and k is the wave number.

3 THE CHBFM FOR THE ACOUSTIC WAVE PROBLEMS

As in the BEM, only the boundary discretisation is required in the BFM based on the Burton-Miller equation (CHBFM) for solving acoustic wave problems. One of the essential differences between BFM and BEM is that boundary elements are built in different spaces, namely, elements used in BFM are located in the two-dimensional parametric space of the bounding surface, while in the BEM elements are located in the three-dimensional physical space. In the BFM, the geometric data over the elements are calculated directly from the surfaces using the following map F:

$$f(x,y,z) = f(x(t_1,t_2), y(t_1,t_2), z(t_1,t_2)) = f(t_1,t_2) \quad x,y,z \in \Omega,\ t_1,t_2 \in \bar{\Omega} \tag{8}$$

where f is the geometric map function of the parametric space to physical surface; t_1 and t_2 are the parametric coordinates which are constrained to the interval [0,1] mostly; Ω is the physical space; and $\bar{\Omega}$ is the parametric space corresponding to Ω. Through the geometric map F, the outward normals at the locations on the boundary, the shape functions and its derivatives can be constructed in the parametric space $\bar{\Omega}$. The detailed description and integration scheme can be found in Qin et al (2010).

To clearly show the differences of the discretisation between the BFM and BEM, their boundary meshes on the same cylinder are shown in figure 1. The elements in BFM (figure 1(a)) keep exact geometry, while the elements in BEM are used to approximate the geometry of the cylinder, thus introduces geometric errors. The geometric errors may lead to accuracy loss, which will be illustrated in the numerical examples in section 4.

By dividing the boundary S into L elements and applying the shape functions on the element, we have the following approximations for variation of pressure and velocity:

$$\phi(P) = \sum_{k=1}^{L} N_k(P)\phi_k = \sum_{k=1}^{L} N_k(t_1,t_2)\phi_k \tag{9}$$

$$q(P) = \sum_{k=1}^{L} N_k(P)q_k = \sum_{k=1}^{L} N_k(t_1,t_2)q_k \tag{10}$$

where ϕ_k and q_k denote the value of ϕ and q at the k^{th} node, respectively; and $N_k(.)$ is the shape function associated with the k^{th} node. If the constant elements are used, we have $N_k(.) = 1$ and $\frac{\partial\phi}{\partial t_\alpha}(P_0) = 0$ ($\alpha = 1, 2$).

We substitute equations (9) and (10) into (7) and the

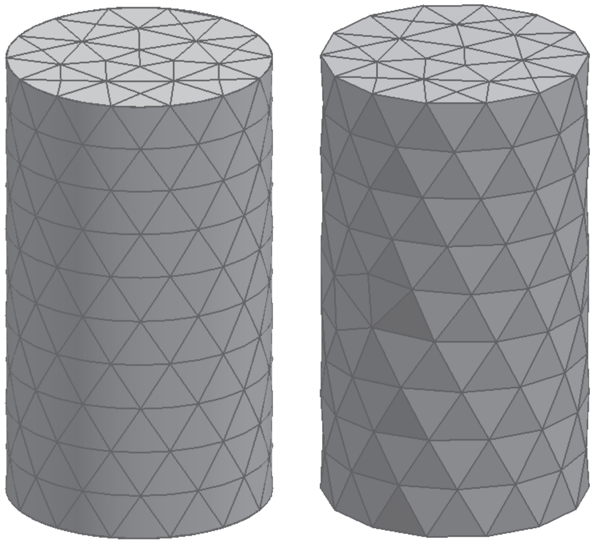
(a) (b)

Figure 1: Two types of boundary discretisations – (a) BFM elements and (b) BEM elements.

following discretised form can be obtained as in equation (11), below, in which $P_0^{\,i}$ denotes the node i.

The outward normal is depicted as:

$$n(t_1,t_2)=\frac{r_{t_1}(t_1,t_2)\times r_{t_2}(t_1,t_2)}{J} \tag{12}$$

where $r_{t_1}(t_1,t_2)$ and $r_{t_2}(t_1,t_2)$ are tangent vectors at the point over the surface, and the two vectors are defined as:

$$r_{t_1}(t_1,t_2)=\frac{\partial r(t_1,t_2)}{\partial t_1}=\left(\frac{\partial x(t_1,t_2)}{\partial t_1},\frac{\partial y(t_1,t_2)}{\partial t_1},\frac{\partial z(t_1,t_2)}{\partial t_1}\right) \tag{13}$$

$$r_{t_2}(t_1,t_2)=\frac{\partial r(t_1,t_2)}{\partial t_2}=\left(\frac{\partial x(t_1,t_2)}{\partial t_2},\frac{\partial y(t_1,t_2)}{\partial t_2},\frac{\partial z(t_1,t_2)}{\partial t_2}\right) \tag{14}$$

$J=\left|r_{t_1}(t_1,t_2)\times r_{t_2}(t_1,t_2)\right|$ is the Jacobian of the geometric map F. In BFM, the normal $n(t_1, t_2)$ and Jacobian J are directly computed from parametric surface rather than from approximation elements as in BEM.

Through section 2 we know that all the integrals in equation (11) have been converted into weakly singular integral forms which can be calculated through the elements directly. The weakly singular treatments in this paper are the same as those in BFM potential analysis. Since each surface element employed in BFM is defined in the parametric space $\bar{\Omega}$, the integrand quantities for each integration point in the physical space Ω can be derived from corresponding parametric surface $\bar{\Omega}$ by the geometric map F, keeping geometric data exact.

Considering the boundary conditions, equation (11) can be put in the following matrix form:

$$\mathbf{A}\mathbf{x}=\mathbf{b} \tag{15}$$

where **b** is the known vector, **x** is an unknown vector to be computed and **A** is the system matrix.

4 NUMERICAL EXAMPLES

The CHBFM has been implemented in a code written in C++ and tested with radiation and scattering problems on three different geometries.

The relative error is defined as following form:

$$error=\frac{1}{|\phi|_{\max}}\sqrt{\frac{1}{N}\sum_{i=1}^{n}(\phi_i^a-\phi_i^r)} \tag{16}$$

where N is the number of the node points; ϕ_i^a and ϕ_i^r are analytical solution and numerical solution at node point i, respectively; and $|\phi|_{\max}$ is the maximum value among the analytical solutions.

4.1 Radiation problems on a cylinder

We start numerical examples with radiation problem on a cylinder domain (figure 2) to verify the accuracy and efficiency of the CHBFM. The radius a of this cylinder is 1, and the length is 5. To get comparative results, the BEM based on the Burton-Miller equation (CHBEM) has also been implemented in code with C++. The pulsating cylinder is formulated by prescribing the normal velocity on a cylinder surface produced by a pulsating sphere with radius of 1. The pulsating sphere is circumscribed by the cylinder. Thus the boundary condition prescribed on the cylinder surface is given as:

$$\begin{aligned}
&\gamma\sum_{k=1}^{L}N_k(P_0^i)\phi_k+\sum_{j=1}^{L}\int_{S_j}\left[\frac{\partial G(P_0^i,P)}{\partial n}-\frac{\partial\bar{G}(P_0^i,P)}{\partial n}\right]\sum_{k=1}^{L}N_k(P)\phi_k dS(P)+\sum_{j=1}^{L}\int_{S_j}\frac{\partial\bar{G}(P_0^i,P)}{\partial n}\sum_{k=1}^{L}(N_k(P)-N_k(P_0^i))\phi_k dS(P)\\
&+\beta\sum_{j=1}^{L}\int_{S_j}\left[\frac{\partial^2G(P_0^i,P)}{\partial n\partial n_0}-\frac{\partial^2\bar{G}(P_0^i,P)}{\partial n\partial n_0}\right]\sum_{k=1}^{L}N_k(P)\phi_k dS(P)+\beta\sum_{j=1}^{L}\int_{S_j}\frac{\partial^2\bar{G}(P_0^i,P)}{\partial n\partial n_0}\sum_{k=1}^{L}[N_k(P)-N_k(P_0^i)]\phi_k dS(P)\\
&=\sum_{j=1}^{L}\int_{S_j}G(P_0^i,P)\sum_{k=1}^{L}N_k(P)q_k dS(P)+\phi^I(P_0^i)+\beta\sum_{j=1}^{L}\int_{S_j}\left[\frac{\partial G(P_0^i,P)}{\partial n_0}+\frac{\partial\bar{G}(P_0^i,P)}{\partial n}\right]\sum_{k=1}^{L}N_k(P)q_k dS(P)\\
&-\beta\sum_{j=1}^{L}\int_{S_j}\frac{\partial\bar{G}(P_0^i,P)}{\partial n}\sum_{k=1}^{L}[N_k(P)-N_k(P_0^i)]q_k dS(P)+\beta\frac{\partial\phi^I(P_0^i)}{\partial n_0}-\gamma\sum_{k=1}^{L}N_k(P_0^i)q_k
\end{aligned} \tag{11}$$

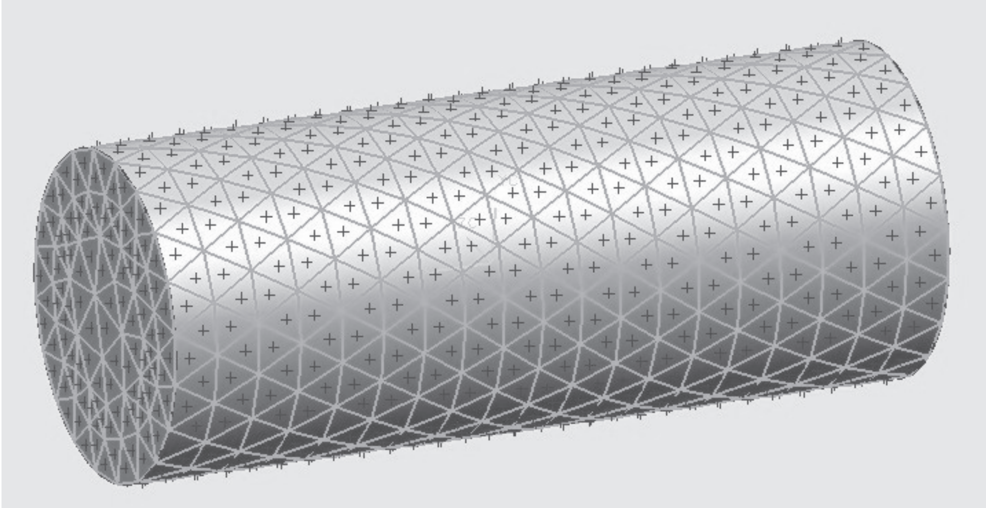

Figure 2: A cylinder model with 972 constant elements.

$$q = -\frac{\partial \phi(r)}{\partial n} \tag{17}$$

where $\phi(r)$ is the sound pressure potential obtained by the pulsating sphere. $\phi(r)$ is expressed as the following simple form:

$$\phi(r) = \frac{e^{ik(r-a)}}{r} \tag{18}$$

This example is similar to one illustrated example by Seybert et al (1985). The relative errors of nodal values of sound pressure obtained by the CHBFM and the CHBEM are shown in figure 3. The comparative results show that the CHBFM has higher accurate results than CHBEM at the same number of elements, regardless of the wave number k = 1 or π (this is a fictitious eigen-frequency for the CBIE). The problem with fictitious frequencies for the CBIE has been circumvented (k = π). Figure 4 shows the total CPU time of each testing case. From this figure, we clearly found that the CPU time used in the CHBFM is almost the same as that of the CHBEM. This numerical example demonstrated that the CHBFM can effectively and accurately solve the radiation problems. The CHBFM out-performs CHBEM on accuracy at the same element number with almost the same CPU time.

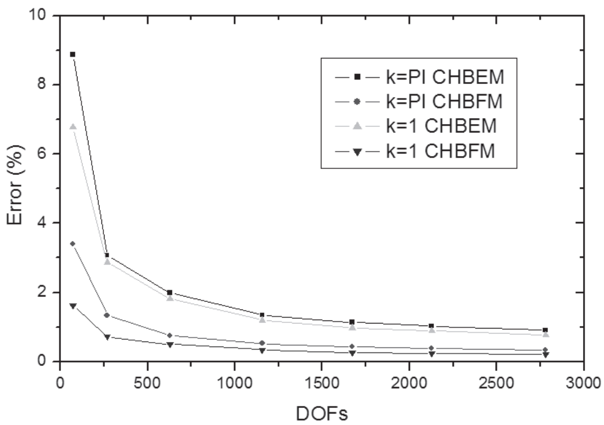

Figure 3: The relative errors of nodal values by the CHBFM and the CHBEM.

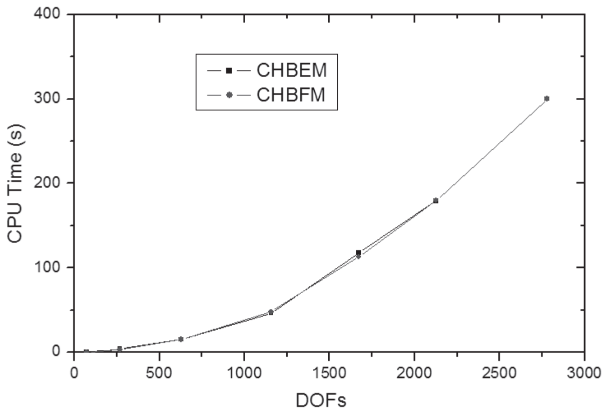

Figure 4: The CPU time used in the CHBEM and the CHBFM.

4.2 Scattering problem on a sphere

A rigid sphere model (figure 5) with radius a = 1 is employed here to verify the CHBFM for scattering problems. The sphere is impinged upon by a unit incoming plane wave in the x direction. The analytical solution for the scattered potential at a distance r from the sphere center and at an angle θ from the direction of the incoming wave is given by (Hickling & Wang, 1966):

$$\phi^s(r,\theta) = \sum_{m=0}^{\infty} -\frac{i^m(2m+1)j_m{}'(ka)}{h_m{}'(ka)} P_m(\cos\theta) h_m(kr) \tag{19}$$

where P_m is the Legendre function of the first kind; h_m denotes the spherical Hankel function of the first kind; and j_m is the spherical Bessel function of the first kind. Figure 6 shows the variation of $|\phi|$ at a radius 4a which is plotted versus the polar angle θ when ka = 1.0. The results are obtained the CHBFM using 136 constant elements. The relative error of the points is 0.04381%. Figure 6 illustrates the computed pressures are much coincide with the analytical solutions. This example has demonstrated that present method can effectively and accurately solve the scattering problems.

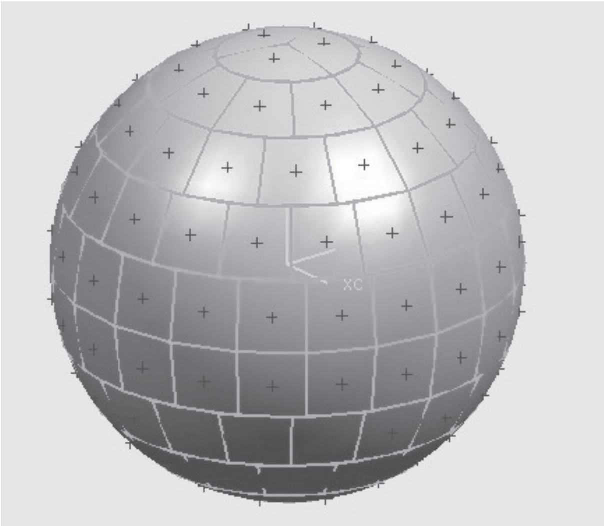

Figure 5: A sphere model with 136 constant elements.

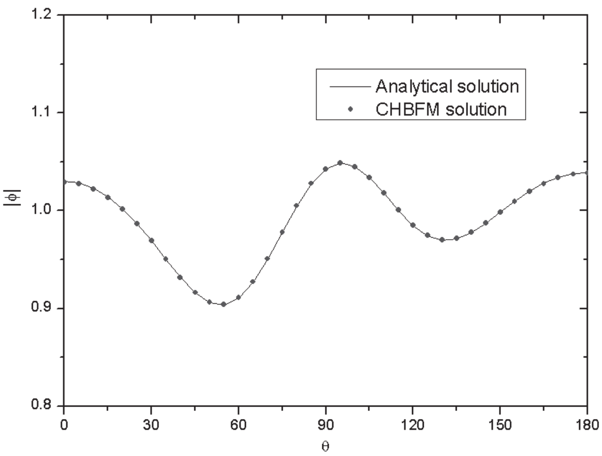

Figure 6: The sound pressure versus polar angle.

4.3 Radiation problem on a complex engineering model

The final example considers the radiation of acoustic wave from an engineering model (figure 7), which is represented with B-rep data structure obtained from the commercial CAD software UG-NX. The overall dimensions of the model are [–0.704, 0.4195]×[–0.444, 0.444]×[–0008, 0.508] in physical space. The boundary condition for the model is a uniform normal velocity $v_0 = 1.0$ on the model surface, and $\partial\phi/\partial n = ik\rho c v_0$ with $k = 1$. The total 6236 elements are used to discretise all surfaces of the model. The evaluation points with total number of 189 are distributed on the sphere surface with radius of 1.0 centred at (0, 0, 0.3). Figure 8 shows the computed sound pressure distribution of this field surface. This example demonstrates that the integration of the CHBFM with the UG-NX is successful, and the CHBFM can effectively analyse the models with complicated geometry.

5 CONCLUSION AND FUTURE WORK

The BFM has been implemented with surface elements on the geometry directly based on the CBIE

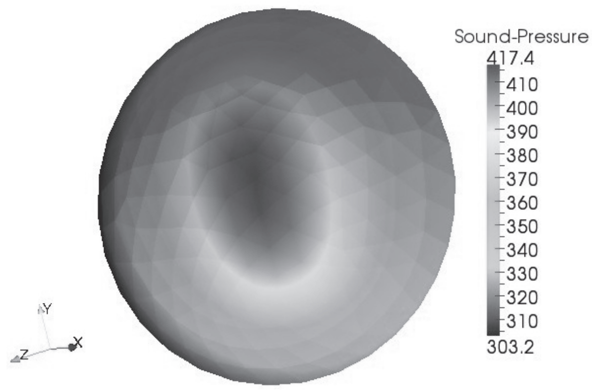

Figure 8: Computed sound pressure distribution on the field surface for the engineering model.

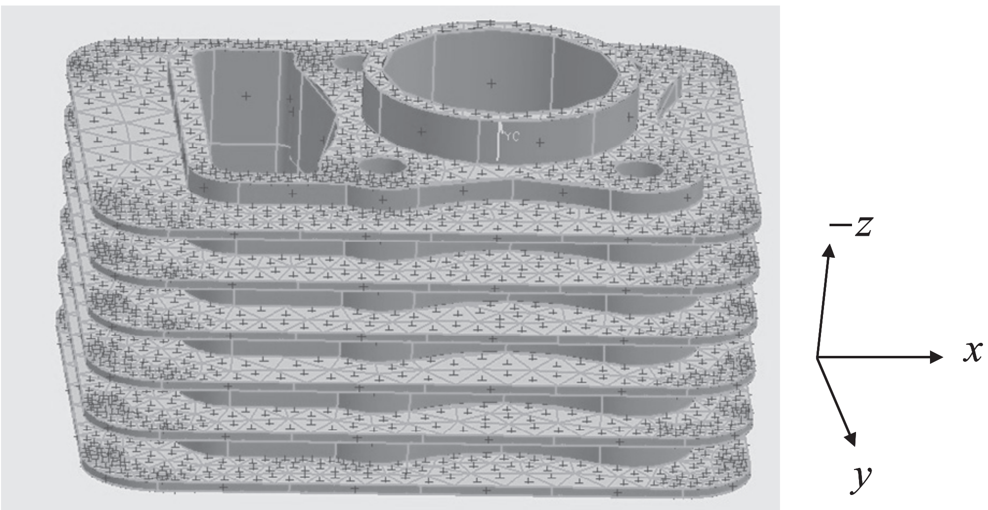

Figure 7: A complex engineering model with 6236 elements.

and HBIE to the radiation and scattering problems of acoustic wave. In the CHBFM, we only need the parameter discretisation of all the boundary surfaces, all the boundary integration and interpolation of the field variables are performed in the parametric space of each boundary face. Thus the geometric errors can be avoided. The CHBFM provides a natural way to integrate geometric design and engineering analysis into a completely unified framework.

In this paper, we employed the parametric constant elements. The numerical examples demonstrated that CHBFM obtained results with better accuracy when compared with the CHBEM. What is more, in the CHBFM all computations are performed directly on the original CAD models, even with complicated geometry.

Application the BFM analysing the models with microscopic characteristics also is a meaningful work. Coupling with fast multi-pole method (Zhang et al, 2005; Shen & Liu, 2007a; 2007b), the BFM can perform large-scale computations for more complicated structures, which is an ongoing work of our research.

ACKNOWLEDGEMENTS

This work was supported by National Science Foundation of China under grant numbers 10972074 and 11172098.

REFERENCES

Benthien, W. & Schenck, H. A. 1997, "Nonexistence and nonuniqueness problems associated with integral equation methods in acoustics", *Comput. Struct.*, Vol. 65, pp. 295-305.

Burton, A. J. & Miller, G. F. 1971, "The application of integral equation methods to numerical solution of some exterior boundary value problem", *Proc. R. Soc. London A*, Vol. 323, pp. 201-210.

Chen, L. H. & Schweikert, D. G. 1963, "Sound radiation from an arbitrary body", *J. Acoust. Soc. Am.*, Vol. 35.

Chien, C. C., Rajiyah, H. & Atluri, S. N. 1990, "An effective method for solving the hypersingular integral equations in 3D acoustics", *J. Acoust. Soc. Am.*, Vol. 88, pp. 918-937.

Chertock, G. 1964, "Sound radiation from vibrating surfaces", *J. Acoust. Soc. Am.*, Vol. 36, pp. 1305-1313.

Gu, J. L., Zhang, J. M., Sheng, X. M. & Li, G. Y. 2011, "B-spline approximation in boundary face method for three-dimensional linear elasticity", *Eng. Anal. Bound. Elem.*, Vol. 35, pp. 1159-1167.

Gu, J. L., Zhang, J. M., Sheng, X. M. & Li, G. Y. 2012, "Isogeometric analysis in BIE for 3-D potential problem", *Eng. Anal. Bound. Elem.*, Vol. 36, pp. 858-865.

Guiggiani, M. 1998, "Formulation and numerical treatment of boundary integral equations with hypersingular kernels", *Singular integrals in boundary element methods*, Sladek, V. & Sladek, J. (editors), Computational Mechanics Publications, Southampton, pp. 85-124.

Hickling, R. & Wang, N. M. 1966, "Scattering of sound by a rigid movable sphere", *J. Acoust. Soc. Am.*, Vol. 39, pp. 276-279.

Jawson, M. A. & Symm, G. T. 1963, "Integral equation methods in potential theory- I, II", *Proc. Royal Soc.*, Vol. 275A, pp. 23-46.

Kleinman, R. E. & Roach, G. F. 1974, "Boundary integral equation for the three-dimensional Helmholtz equation", *SIAM REV.*, Vol. 16, pp. 214-236.

Lee, C. H. & Sclavounos, P. D. 1989, "Removing the irregular frequencies from integral equations in wave-body interactions", *J. Fluid Mech.*, Vol. 207, pp. 393-418.

Li, S. & Huang, Q. 2010, "An improved form of the hypersingular boundary integral equation for exterior acoustic problems", *Eng. Anal. Bound. Elem.*, Vol. 34, pp. 189-195.

Liu, Y. J. & Chen, S. H. 1999, "A new form of the hyper-singular boundary integral equation for 3-D acoustics and its implementation with C0 boundary element", *Comput. Methods Appl. Mech. Eng.*, Vol. 173, pp. 375-386.

Liu, Y. J. & Rizzo, F. J. 1992, "A weakly-singular form of the hypersingular boundary integral equation applied the 3D acoustic wave problem", *Comput. Method Appl. Mech. Eng.*, Vol. 96, pp. 271-287.

Liu, Y. J. & Rudolphi, T. J. 1991, "Some identities for fundamental solutions and their applications to non-singular boundary element formulations", *Eng. Anal. Bound. Elem.*, Vol. 8, pp. 301-311.

Liu, Y. J. & Rudolphi, T. J. 1999, "New identities for fundamental solutions and their applications to non-singular boundary element formulations", *Comput. Mech.*, Vol. 24, pp. 286-292.

Matsumoto, T., Zheng, C. J., Harada, S. & Takahashi, T. 2010, "Explicit evaluation of hypersingular boundary integral equation for 3-D Helmholtz equation discretized with constant triangular element", *J. Comput. Sci. Eng.*, Vol. 4, pp. 194-206.

Meyer, W. L., Bell, W. A., Stallybrass, M. P. & Zinn, B. T. 1979, "Prediction of the sound field radiated from axisymmetric surfaces", *J. Acoust. Soc. Am.*, Vol. 65, pp. 631-638.

Qin, X. Y., Zhang, J. M., Li, G. Y., Sheng, X. M., Song, Q. & Mu, D. H. 2010, "An element implementation of the boundary face method for potential problems in three dimensions", *Eng. Anal. Bound. Elem.*, Vol. 34, pp. 934-943.

Rudolphi, T. J. 1991, "The use of simple solutions in the regularization of hypersingular boundary integral equations", *Math. Comput. Model*, Vol. 15, pp. 269-278.

Schenck, H. A. 1968, "Improved integral formulation for the acoustic radiation problem", *J. Acoust. Soc. Am.*, Vol. 44, pp. 41-58.

Segalman, D. J. & Lobitz, D. W. 1992, "A method to overcome computational difficulties in the exterior acoustic problems", *J. Acoust. Soc. Am.*, Vol. 91, pp. 1855-1861.

Seybert, A. F. & Rengarajan, T. K. 1987, "The use of CHIEF to obtain unique solution for acoustic radiation using boundary integral equations", *J. Acoust. Soc. Am.*, Vol. 81, pp. 1299-1306.

Seybert, A. F., Soenarko, B., Rizzo, F. J. & Shippy, D. J. 1985, "An advanced computational method for radiation and scattering of acoustic waves in three dimensions", *J. Acoust. Soc. Am.*, Vol. 77, pp. 362-368.

Shen, L. & Liu, Y. J. 2007a, "An adaptive fast multipole boundary element method for three-dimensional potential problems", *Comput. Mech.*, Vol. 39, pp. 681-691.

Shen, L. & Liu, Y. J. 2007b, "An adaptive fast multipole boundary element method for three dimensional acoustic wave problems based on the Burton-Miller formulation", *Comput. Mech.*, Vol. 40, pp. 461-472.

Wu, T. W. & Seybert, A. F. 1991, "A weighted residual formulation for the CHIEF method in acoustics", *J. Acoust. Soc. Am.*, Vol. 90, pp. 1608-1614.

Zhang, J. M. 2010, "Theory and application of stress analysis on complete solids based on boundary face method", *Computer Aided Engineering*, Vol. 19, pp. 5-10.

Zhang, J. M., Tanaka, M. & Endo, M. 2005, "The hybrid boundary node method accelerated by fast multipole expansion technique for 3D potential problems", *Int. J. Num. Meth. Eng.*, Vol. 63, pp. 660-680.

Zhang, J. M., Qin, X. Y., Han, X. & Li, G. Y. 2009, "A boundary face method for potential problems in three dimensions", *Int. J. Numer. Meth. Eng.*, Vol. 80, pp. 320-337.

Zhou, F. L., Zhang, J. M., Sheng, X. M. & Li, G. Y. 2011, "Shape variable radial basis function and its application in dual reciprocity boundary face method", *Eng. Anal. Bound. Elem.*, Vol. 35, pp. 244-252.

XIANHUI WANG

Xianhui Wang received his BE and MS from the College of Mathematics and Econometrics, Hunan University, China, in 2007 and 2009, respectively. He is currently working toward his PhD at the College of Mechanical and Vehicle Engineering, Hunan University, China. His research activities are concerned with numerical methods for acoustics problems and the boundary integral equation method.

JIANMING ZHANG

Jianming Zhang received his PhD in engineering mechanics from Tsinghua University, China, in 2002. He then started postdoctoral research at Shinshu University, Japan, with Prof Masataka Tanaka. He became a JSPS fellow in 2005, and the research was funded until he joined Hunan University, China, in 2007. Since 2007, he has been employed as a professor in college of mechanical and vehicle engineering at Hunan University. He has been engaged in research of the boundary integral equation method and its applications in engineering problems.

FENGLIN ZHOU

Fenglin Zhou received his BE degree in information and computation science from Beijing Jiaotong University, China, in 2008. He is currently working toward his PhD at the College of Mechanical and Vehicle Engineering, Hunan University, China. His research activities are concerned with numerical methods for heat transfer problem and the boundary integral equation method.